Direct Observation of the Mott Transition in an Optically Excited Semiconductor Quantum Well

L. Kappei, J. Szczytko, F. Morier-Genoud, and B. Deveaud
Ecole Polytechnique Fédérale de Lausanne, EPFL, CH-1015 Lausanne, Switzerland
(Received 22 July 2004; published 15 April 2005)

We have studied density-dependent time-resolved photoluminescence from a 80 Å InGaAs/GaAs single quantum well excited by picosecond pulses. We succeed in giving evidence for the transition from an exciton-dominated population to an unbound electron-hole pair population as the pair density increases. For pair densities below this excitonic Mott transition we observe a spectrally separate emission from free electron-hole pairs in addition to excitonic luminescence, thereby proving the coexistence of both species. Exciton binding energy and band gap remain unchanged even near the upper bound of this coexistence region. Above the Mott density we observe a purely exponential high energy tail of the photoluminescence and a redshift of the band gap with pair density. The transition occurs gradually between 1×10^{10} and 1×10^{11} cm^{-2} at the carrier temperatures of our experiment.

DOI: 10.1103/PhysRevLett.94.147403 PACS numbers: 78.67.De, 71.10.Hf, 71.35.Cc, 78.47.+p

The idea of a metal insulator transition, when either the density of carriers or their Coulomb correlation are changed, was put forward by Mott in a seminal paper [1], and has been very actively studied since [2]. Both the theoretical aspects and the experimental observations have been subject to active discussion over the last 40 years in the different branches of solid state physics where this type of transition may appear. One of the cases of interest, amongst many others, is the case of an optically excited semiconductor where the theory predicts a transition from an insulating exciton gas at low densities to a conducting electron-hole plasma at high densities. Some reports discuss possible observations of such a transition [3–5]; they are, however, rather elusive despite the very clear interest that such an observation would raise. Recently, Nozières pointed out [6] that we are still lacking appropriate experimental information about the properties of the Mott transition in semiconductors under optical excitation. Quoting his own words: ''we need simple and clear experimental information.''

The difficulties in getting simple and clear information on the Mott transition through interband optical excitation resides in a number of problems, which add up in most experimental configurations. A bulk sample should not be used, just because of the inhomogeneous excitation generated by the finite absorption coefficient of the sample that prevents getting a well-defined pair density. In the same way, a sample with several quantum wells cannot be used, and a proper imaging of the emitted luminescence has to be realized in order to define precisely the density of pairs. Then a precise signature of the two different phases has to be found, such as, for example, the infrared conductivity of the sample proposed by Nagai *et al.* [4] for the conducting phase in the case of CuCl or the Terahertz absorption for the exciton phase, as proposed by Kaindl *et al.* [7].

In this Letter, we show that a sample of sufficient quality allows measurable differences in the interband luminescence between the exciton phase and the free-carrier plasma, which provide a very simple way to probe the Mott transition. We observe a gradual transition from one phase to the other as a function of the pair density between 1×10^{10} and 1×10^{11} cm^{-2}. We also evidence the absence of any shift of the exciton energy and the gap energy, a finding which contradicts available theories. Above the Mott density, a redshift of the lower edge of the luminescence line and a blueshift of the upper edge are observed, corresponding to the expected signatures of band gap renormalization and Fermi filling, respectively.

The sample contains a single 80 Å $In_xGa_{1-x}As$ quantum well (QW), with a low indium content of 5% grown by molecular-beam epitaxy. This QW is embedded in the middle of a GaAs layer of total mean thickness λ (where λ corresponds to the wavelength of the excitonic resonance in the QW), which was grown over a 10 period distributed Bragg reflector (DBR). The DBR allows us to measure the sample absorption in the reflection configuration without any sample preparation. We refer the reader to [8–10] for an in-depth coverage of the sample characterization. An important sample quality is the low inhomogeneous broadening of the exciton line. As a consequence, the luminescence of the free carriers, setting in about 7 meV above the excitonic resonance, is not masked by the strong exciton line. The separate visibility of excitonic and free-carrier PL permits us to obtain the band gap as well as the exciton binding energy directly from the photoluminescence (PL) spectra.

The sample is optically excited by means of a Ti:sapphire laser delivering picosecond pulses at a photon energy of 1.57 eV corresponding to 80 meV above the QW band gap. The spectral pulse width is 1 meV. The PL from the sample is analyzed using a streak camera in photon counting mode preceded by a monochromator. The spectral and temporal resolution is 0.4 meV and 40 ps, respectively. The laser is focused to a spot of 65 μm (FWHM) on the sample. The sample surface is imaged with a magnification of 3.75 on a pinhole of diameter 50 μm collecting

only light from the excitation spot center. Thus the variation of excitation intensity over the collection region is below 5%.

Figure 1 shows PL spectra integrated from 130 to 180 ps after excitation using various excitation powers. The electron-hole pair density values given in the figure caption have been extracted from a line-shape fit for the highest density. The pair density at lower excitation was assumed to scale linearly with the excitation power. The underlying theoretical model for the line-shape fit is outlined below.

At low excitation density there is no shift with respect to the absorption spectrum confirming the high sample quality. For densities up to $\approx 1 \times 10^{10}$ cm^{-2} we can easily distinguish the free-carrier luminescence appearing at the band gap around 6.5 meV above the 1 s exciton resonance. It displays an exponential decrease to higher energy corresponding to a Boltzmann distribution of the carriers in the bands. The relative magnitude of the exciton and free-carrier luminescence components remains approximately constant in the density range of the first two spectra. Knowing that the free-carrier emission rate is bimolecular, this observation indicates a decrease of the excitonic ionization degree with increasing pair density in this density regime, as predicted by the Saha equation, a mass-action law describing the equilibrium concentration of a gas of coexisting excitons and free carriers [11,12].

At higher pair densities (between 2×10^{10} cm^{-2} and 1×10^{11} cm^{-2}) the exciton as well as the continuum luminescence progressively broaden masking the onset of band-to-band transitions. However, the spectra in this pair density regime still display an excitonic resonance revealed by the nonexponential high-energy tail. At higher density (1.6×10^{11} cm^{-2}) the excitonic resonance completely disappears, evidenced by an exponential high-energy PL tail which is the signature of the emission of a nondegenerate *e-h* plasma. This transition is accompanied by a redshift of the peak emission. The two spectra with highest pair density in Fig. 1 are typical for the emission from a degenerate plasma.

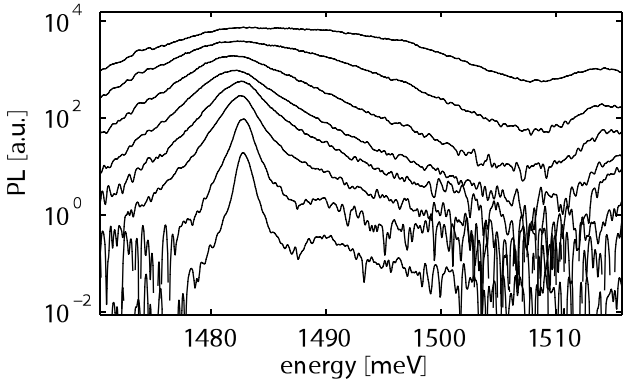

FIG. 1. Spectra for different excitation powers integrated between 130 and 180 ps after excitation. Peak intensities are equally spaced for improved readability. The carrier densities are (from lower to upper curve): 1.6×10^9 cm^{-2}, 7.8×10^9 cm^{-2}, 2.3×10^{10} cm^{-2}, 4.7×10^{10} cm^{-2}, 7.8×10^{10} cm^{-2}, 1.6×10^{11} cm^{-2}, 3.1×10^{11} cm^{-2}, and 6.2×10^{11} cm^{-2}.

The carrier density was determined by applying a line-shape fit to the spectrum of the highest achieved density. The form of the PL signal was calculated assuming parabolic quantum well subbands and considering only transitions between conduction and valence subband states of equal subband indices and identical wave vector $\mathbf{k}$ [13]. The transition matrix elements are assumed to be energy independent and are chosen for TE polarization with the light-hole transition matrix elements being one third of the heavy-hole transition matrix elements. To account for the lifetime broadening mainly due to carrier-carrier scattering, we utilized a Lorentzian broadening of the Landsberg type [14–16], which is implemented by convoluting the unbroadened spectrum $L(E)$ with a Lorentzian of width

$$\Gamma(E) = \Gamma_0 \left[1 - 2.23 \frac{E}{E_F} + 1.46 \left(\frac{E}{E_F} \right)^2 - 0.23 \left(\frac{E}{E_F} \right)^3 \right],$$

where $E = \hbar\omega - E_{\mathrm{gap}}$ is counted from the quantum well band gap E_{gap} and E_F corresponds to the separation of the electron and hole quasi-Fermi levels. The fit parameters are the pair density, the carrier temperature, the broadening factor at the band gap Γ_0, the quantum well band gap, and a normalization constant to match experimental and calculated amplitudes. They are determined by a least-square fit of the logarithms of calculated and measured curves. Examples of fits are shown as crosses in Fig. 2(a). The broadening Γ_0 at the band gap varied from 9.5 meV at a delay of 75 ps to 2.3 meV at a delay of 560 ps. The uncertainty in the extracted pair density values at early delay times is estimated to be $\pm 10\%$. In this high-density regime, the spectral width of the spectrum is much larger than the one-particle broadening visible at the low-energy edge of the emission. Thus, the spectral width is essentially determined by the pair density, explaining the relatively low error limits at high density. These uncertainty limits equally apply to density values given for lower excitation intensity, which are calculated according to the respective fraction of excitation intensity. The effective mass values m^* used in these calculations were $m_{\mathrm{e}}^* = 0.08 m_{\mathrm{e}}$ for electrons and $m_{\mathrm{hh}}^* = 0.5 m_{\mathrm{e}} / m_{\mathrm{lh}}^* = 0.08 m_{\mathrm{e}}$ for heavy or light holes.

Figure 2(a) shows spectra at different delay times at the highest pair density reached in our experiment. The crosses show line-shape fits calculated as outlined above. The density obtained from the fits is displayed in Fig. 2(b) as a function of delay time (circles). The spectral shape of the emission changes from a broad plasma emission with a quasiconstant intensity over 15 meV at a delay of 110 ps towards an excitonic emission at 1830 ps of delay. The saturation of the intensity at early delays is a direct evidence of *k*-space filling and of the *k*-selection rule for an *e-h* plasma [17]. At a delay time of approximately 800 ps we still have a purely exponential high-energy tail of the

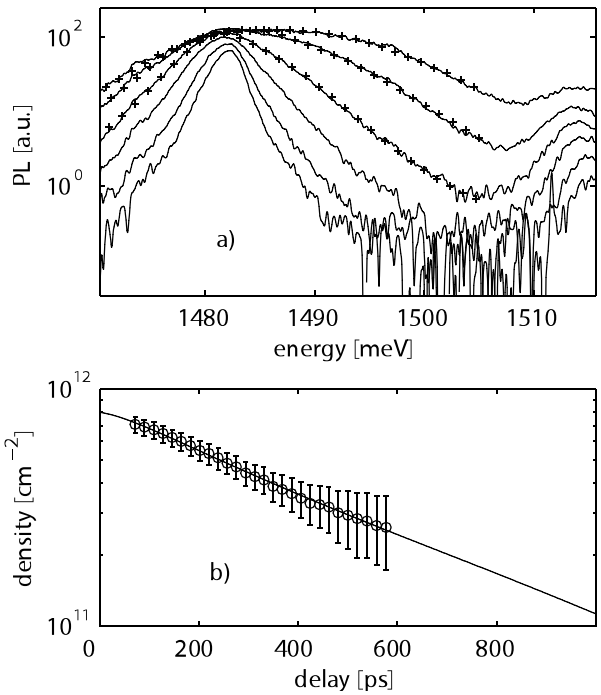

FIG. 2. (a) Spectra at the highest used excitation power (8 mW) at different delay times. The delay times are 110 ps, 270 ps, 520 ps, 830 ps, 1330 ps, and 1830 ps from upper to lower on the right side of the graph. Crosses: fit to the experimental spectra. (b) Circles: extracted pair density obtained by applying a line-shape fit to the spectra. For delays beyond 600 ps, the fit does not converge due to the excitonic enhancement not being included in the above PL line-shape model. Solid line: $B - A \int Pdt$ (as explained in the text).

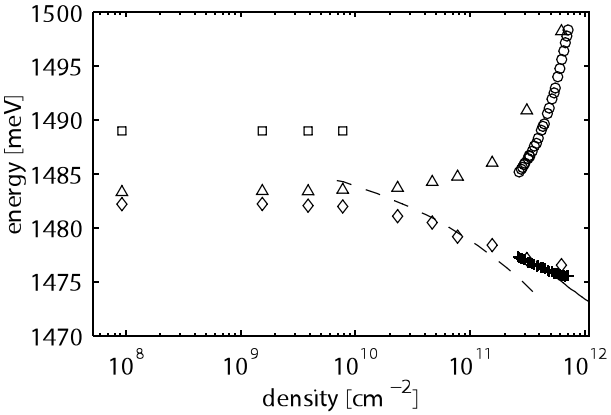

FIG. 3. Spectral features of the PL at various excitation powers. Diamonds: low-energy edge (half maximum); triangles: high-energy edge (half maximum); squares: free-carrier PL maxima; crosses: band gap as a fit parameter from the fitting procedure of the highest excitation image; circles: Fermi-level separation extracted from the fitting procedure of the highest excitation image; solid line: band gap following the calculation in [18]; dashed line: band gap following calculation in [19].

spectrum evidencing the absence of an excitonic enhancement. At this delay we deduce a density of 1.7×10^{11} cm^{-2} as indicated by the solid line shown in Fig. 2(b). It displays the integral $B - A \int Pdt$ (P is the spectrally integrated intensity), where A and B are chosen to best reproduce the extracted density from the fits. This can be justified if the collection efficiency is regarded as being time independent because in this case the rate of recombining e-h pairs is directly proportional to P. At delays beyond 1000 ps we observe an increasing peaking of the emission at the exciton emission energy. This nonexponential high-energy tail and the continuous reduction of the linewidth at these longer delays evidence the transformation towards an exciton-dominated spectrum [8].

Figure 3 displays the variations of the different spectral features as a function of pair density. Triangles and diamonds display the high- and low-energy edges at half maximum of the main luminescence peak. At low densities, these mark the boundaries to the exciton energy. At high pair densities, these energies roughly scale with the gap position (low-energy edge) and the Fermi energy (high energy). Indeed, the results of our simple line-shape fit (crosses and circles) and of this very direct determination technique do coincide at elevated density. Figure 3 also shows the position of the edge of band-to-band transitions in the low-density regime (squares). The corresponding spectra are extracted from spectral profiles integrated between 130 and 180 ps after excitation with various powers. Pair density values were calculated according to the procedure described above for Fig. 1.

The spectral position of the onset of free-carrier luminescence does not shift as long as it is still clearly visible up to a density of 1×10^{10} cm^{-2}. Already at 1.6×10^{11} cm^{-2} the emission is characteristic for a nondegenerate plasma (see Fig. 1) with a renormalized band gap slightly below the low-density exciton resonance. These two bounds determine the density range in which the transition from a dominantly excitonic population to a gas of unbound carriers takes place.

The solid line in Fig. 3 displays the band gap energy variations based on calculations of Bongiovanni and Staehli [18] for an electron-hole plasma at a temperature of 100 K and scaled with the appropriate exciton binding energy of 6.5 meV. The absolute value is in very good agreement with our measurements. The discrepancy between the steep evolution of the calculated curve and the experimental one has also been observed by the above cited authors and was ascribed to the strong heating at elevated densities decreasing the band gap renormalization. The dashed line shows the band gap calculated by Ando *et al.* [19] for a 145 Å well of GaAs/$Ga_{0.56}Al_{0.44}As$. The results have also been scaled with the proper effective excitonic Rydberg and manifest the discrepancy with our determination of the gap at a pair density below 1×10^{10} cm^{-2}.

Figure 4 shows the temporal evolution of the spectrally integrated PL with various initial excitation powers. There

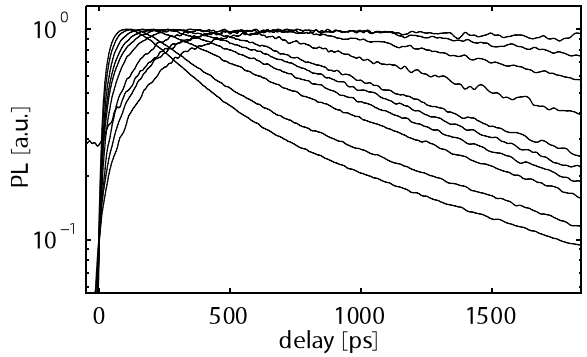

FIG. 4. Normalized decay curves of the total integrated intensity as a function of delay time for various excitation powers. The initial densities correspond to (from lower to upper on the right side of the figure) 8×10^{11}, 4×10^{11}, 2×10^{11}, 1×10^{11}, 6×10^{10}, 3×10^{10}, 1×10^{10}, 5×10^{9}, 2×10^{9}, 1×10^{8} cm^{-2}.

are three different regimes visible in the graph. At very low power the excitonic PL takes hundreds of picoseconds to reach its maximum and subsequently decays very slowly. This behavior is due to the very slow radiative recombination of free carriers and the slow formation of excitons at these low densities. Increasing the excitation power results in a decrease of the PL lifetime due to the increased exciton formation efficiency and the increasing fraction of excitons with respect to the total pair population. Once the bimolecular exciton formation rate is considerably stronger than the radiative recombination rate of the exciton, the PL lifetime remains approximately constant in a large interval of densities. This is due to the predominantly excitonic population (according to the Saha equation, 70% of the total pair population of density 3×10^{10} cm^{-2} are excitons at $T = 30$ K). At the highest densities there is another shortening of the PL lifetime at early delay times. At very short delay times this can be assigned to the fast radiative decay of a degenerate electron-hole plasma.

In conclusion, the Mott transition does not become manifest in an abrupt change of either the spectral form of the emission nor in the evolution of the emitted intensity. It seems to indicate that the Mott transition at least in our kind of transient measurements is rather gradual. One reason for this behavior might be the limited time available to reach equilibrium.

The ensemble of our measurements allows us to determine the density range in which the Mott transition occurs. At low density up to 1×10^{10} cm^{-2} we observe spectra dominated by excitonic transitions and a separately visible spectral component due to free-carrier transitions. At high density in excess of 1.6×10^{11} cm^{-2} we observe pure free-carrier transitions with a band gap below the low-density exciton line. The Mott transition has to occur between these two limits.

On the low-density side of the transition, we do not observe any lowering of the band gap energy or the exciton binding energy up to 1×10^{10} cm^{-2}, which contradicts theoretical expectations [19–21]. However, we see a band gap reduction due to many-body effects on the high-density side of the transition which is in agreement with previous work.

We would like to thank J.-L. Staehli and J.-D. Ganière for fruitful discussions and acknowledge financial support from the Swiss National Science foundation.

[1] N. F. Mott, Proc. Phys. Soc. London **62**, 416 (1949).
[2] N. F. Mott, *Metal Insulator Transitions* (Taylor & Francis, London, 1990), 2nd ed.
[3] J. Shah, M. Combescot, and A. Dayem, Phys. Rev. Lett. **38**, 1497 (1977).
[4] M. Nagai and M. Kuwata-Gonokami, J. Lumin. **100**, 233 (2002).
[5] H. Yoon, M. Sturge, and L. Pfeiffer, Solid State Commun. **104**, 287 (1997).
[6] P. Nozières, Ann. Phys. Coll. C2 **20**, 417 (1995).
[7] R. Kaindl, M. Carnahan, D. Hägele, R. Lövenich, and D. Chemla, Nature (London) **423**, 734 (2003).
[8] J. Szczytko, L. Kappei, J. Berney, F. Morier-Genoud, M. Portella-Oberli, and B. Deveaud, Phys. Rev. Lett. **93**, 137401 (2004).
[9] J. Szczytko, L. Kappei, F. Morier-Genoud, T. Guillet, M. Portella-Oberli, and B. Deveaud, Phys. Status Solidi C **1**, 493 (2004).
[10] J. Szczytko, L. Kappei, J. Berney, F. Morier-Genoud, M. Portella-Oberli, and B. Deveaud, Phys. Rev. B (to be published).
[11] R. Zimmermann, *Many-Particle Theory of Highly Excited Semiconductors* (Teubner-Verlag, Leipzig, 1988).
[12] D. Robart, X. Marie, B. Baylac, T. Amand, M. Brousseau, G. Bacquet, G. Debart, R. Planel, and J. Gerard, Solid State Commun. **95**, 287 (1995).
[13] S. Chuang, *Physics of Optoelectronic Devices* (Wiley, New York, 1995).
[14] R. Martin and H. Störmer, Solid State Commun. **22**, 523 (1977).
[15] E. Zielinski, H. Schweizer, S. Hausser, R. Stuber, M. Pilkuhn, and G. Weimann, IEEE J. Quantum Electron. **23**, 969 (1987).
[16] P. Landsberg, Phys. Status Solidi **15**, 623 (1966).
[17] B. Deveaud *et al.*, Appl. Phys. Lett. **55**, 2646 (1989).
[18] G. Bongiovanni and J.-L. Staehli, Phys. Rev. B **39**, 8359 (1989).
[19] T. Ando, M. Nakayama, and M. Hosoda, Phys. Rev. B **69**, 165316 (2004).
[20] N. B. B. Aouani, L. Mandhour, R. Bennaceur, S. Jaziri, T. Amand, and X. Marie, Solid State Commun. **108**, 199 (1998).
[21] H. Reinholz, Solid State Commun. **123**, 489 (2002).